Application of the χ^2 principle and unbiased predictive risk estimator for determining the regularization parameter in 3D focusing gravity inversion

Saeed Vatankhah[1], Vahid E Ardestani[1] and Rosemary A Renaut[2]
[1]Institute of Geophysics, University of Tehran, Tehran, Iran
[2] School of Mathematical and Statistical Sciences, Arizona State University, Tempe, US

August 5, 2014

Abstract

The χ^2 principle and the unbiased predictive risk estimator are used to determine optimal regularization parameters in the context of 3D focusing gravity inversion with the minimum support stabilizer. At each iteration of the focusing inversion the minimum support stabilizer is determined and then the fidelity term is updated using the standard form transformation. Solution of the resulting Tikhonov functional is found efficiently using the singular value decomposition of the transformed model matrix, which also provides for efficient determination of the updated regularization parameter each step. Experimental 3D simulations using synthetic data of a dipping dike and a cube anomaly demonstrate that both parameter estimation techniques outperform the Morozov discrepancy principle for determining the regularization parameter. Smaller relative errors of the reconstructed models are obtained with fewer iterations. Data acquired over the Gotvand dam site in the south-west of Iran are used to validate use of the methods for inversion of practical data and provide good estimates of anomalous structures within the subsurface.

Keywords: Inverse theory; Numerical approximations and analysis; Tomography; Gravity anomalies and Earth structure; Asia

1 Introduction

Gravity surveys have been used for many years for a wide range of studies including oil and gas exploration, mining applications, mapping bedrock topography, estimation of the crustal thickness and recently-developed microgravity investigations [14]. The inversion of gravity data is one of the important steps in the interpretation of practical data. The goal is to estimate density and geometry parameters of an unknown subsurface model from a set of

known gravity observations measured on the surface. In the linear inversion of gravity data it is standard to assume that the subsurface under the survey area can be approximated through a discretization of the subsurface into rectangular blocks of constant density [3]. In solving for the densities at these blocks this kind of parameterization is flexible for the reconstruction of the subsurface model, but requires more unknowns than observations and thus introduces algebraic ambiguity in the solution of the linear system. Additionally, the existence of noise in the measurements of practical data and the inherent non-uniqueness of the gravity sources, based on Gauss's theorem, means that the inversion of gravity data is an example of an underdetermined and ill-posed problem. Thus, in order to find an acceptable solution which is less sensitive to the measurement error regularization, also known as stabilization, is typically imposed. A popular approach uses the minimization of a cost functional that combines the data fidelity with an L2, or Tikhonov, type regularization, see e.g. [2, 7, 20]. Two important aspects of the Tikhonov regularization are the choices of the stabilizing operator and the regularization parameter. The former impacts the class of solution which will be obtained, and the latter controls the trade off between the data fit and the regularization term. Two main classes of stabilizer have been used in the inversion of gravity data; a smoothing stabilizer which employs the first or second derivative of the model parameters see e.g. [10, 3] and a stabilizer which produces non-smooth models e.g. [3, 9, 16]. In this paper the minimum support (MS) stabilizer which was introduced in [9] and developed in [16] is used to reconstruct models with non-smooth features.

The determination of an optimal regularization parameter in potential field data inversion is a topic of much previous research and includes methods such as the L-curve (LC) [11, 4, 18], generalized cross validation (GCV) [4, 18] and the more often adopted Morozov discrepancy principle (MDP) [13, 10, 4]. Because it is well-know that the MDP generally overestimates the regularization parameter, hence leading to overly smoothed solutions, we discuss here regularization parameter estimation in the specific context of the inversion of underdetermined gravity data using the Unbiased Predictive Risk Estimator (UPRE) and the χ^2 principle, see e.g. [20, 19]. Whereas in [18] we considered the use of the GCV and LC methods for 2D focusing inversion, our subsequent investigations in [19] demonstrated that for small scale 2D problems the UPRE and χ^2 principle improve on results using the LC, GCV and MDP, with respect to reduced relative error, reduced computational cost or both. Indeed, all methods demonstrated their efficiency as compared with the MDP [19], but the UPRE and χ^2 techniques offer the most promise for parameter estimation in terms of cost and accuracy. We, therefore, solve the underlying regularized model, with these parameter-choice methods, here contrasting for completeness with the MDP. Moreover, in place of the use of the generalized singular value decomposition (GSVD), [15], as advocated in [18, 19], we use the singular value decomposition (SVD) of the system matrix in standard form [6]. This provides a more efficient tool as compared to the GSVD for the solution of Tikhonov regularized problems of small to moderate scale.

The outline of this paper is as follows. In section 2 we review the derivation of the analytic calculation of the gravity anomaly derived from a 3D cell model. In section 3 the algorithm for focusing inversion is discussed. Furthermore, in this section numerical solutions of the

Tikhonov objective function using the SVD for the regularized-modified model system are discussed. Extensions of the MDP, UPRE and χ^2 methods for estimating the regularization parameter have been extensively discussed in [19], but we provide a brief rationale for the latter two methods which are not well-known in this field in section 4 with necessary formulae collected in B. Results for synthetic examples are illustrated in section 5. The approach is applied on gravity data acquired from Gotvand dam site in section 6. Conclusions and a discussion of future plans follow in section 7.

2 Gravity modelling

Rectangular grid cells are commonly used for 3-D modelling of gravity sources. The subsurface under the survey area is divided into prisms of known sizes and positions. The unknown density contrasts within each prism define the parameters to be estimated. Fig. 1 illustrates the discretization of the subsurface by rectangular prisms. Gravity stations are located at the centers of the upper faces of the prisms in the top layer. The cells are of equal size in each dimension, $\Delta x = \Delta y = \Delta z$ where $\Delta\cdot$ is the distance between gravity stations. Extra cells may be added around the gravity data grid to reduce possible distortions in the reconstruction along the boundary [3].

The vertical component of the gravitational attraction g_i of a prism at point (x_i, y_i, z_i) is given by, [3]

$$\frac{g_i}{\rho_j} = -\Gamma \sum_{p=1}^{2}\sum_{l=1}^{2}\sum_{s=1}^{2} \mu_{pls}\left[a_p \ln\left(b_l + r_{pls}\right) + b_l \ln\left(a_p + r_{pls}\right) - c_s \arctan\left(\frac{a_p b_l}{c_s r_{pls}}\right)\right], \quad (1)$$

with

$$\mu_{pls} = (-1)^p (-1)^l (-1)^s \quad r_{pls} = \left(a_p^2 + b_l^2 + c_s^2\right)^{\frac{1}{2}} \quad \text{and} \quad (2)$$

$$a_p = x_i - x'_p, \quad b_l = y_i - y'_l, \quad c_s = z_i - z'_s, \quad p, l, s = 1, 2. \quad (3)$$

The coordinates of the eight corners for prism j are denoted by (x'_p, y'_l, z'_s). In (1) Γ is the universal gravitational constant, ρ_j is the density of the jth prism and r_{pls} is the distance between one corner of the prism and the observation point. The term on the right-hand side of (1), which quantifies the contribution to the ith datum of unit density in the jth cell, is denoted by the kernel weight G_{ij}, and is valid only at station i for cell j. The total response for station i is obtained by summing over all cells giving

$$g_i = \sum_{j=1}^{n} G_{ij}\rho_j, \quad i = 1, \ldots, m, \quad (4)$$

leading to the linear equation

$$\mathbf{d} = G\mathbf{m}, \quad m \ll n \quad (5)$$

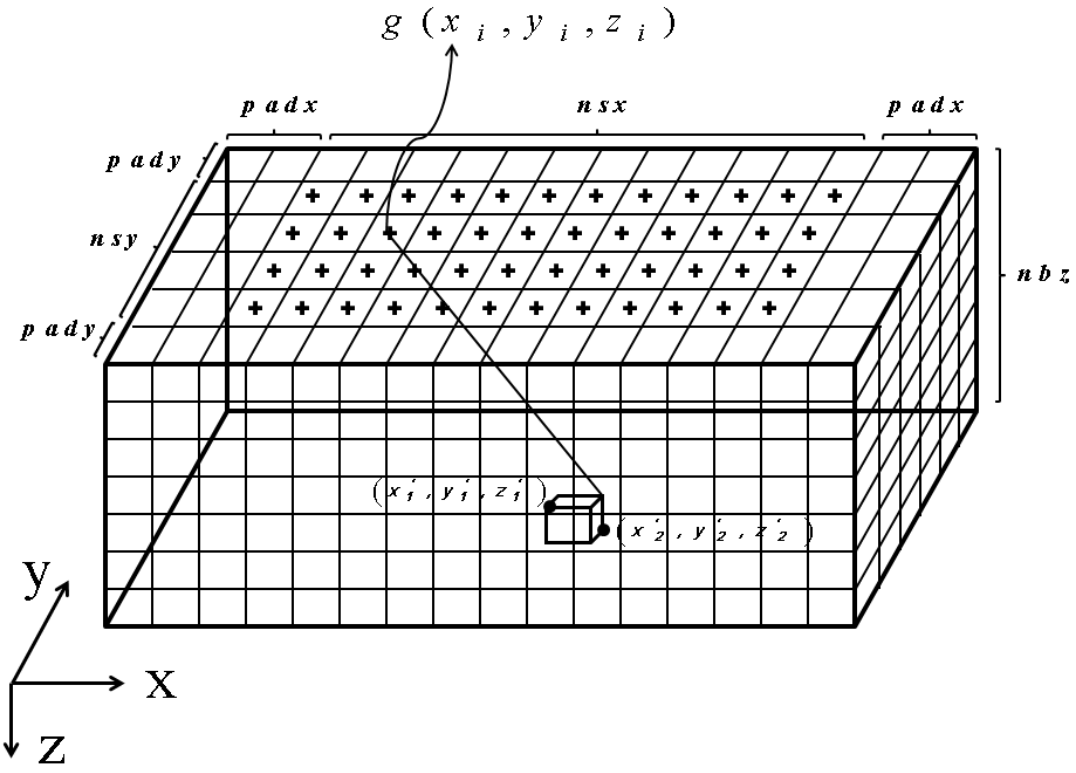

Figure 1: Discretization of the subsurface by rectangular prisms. nsx, and nsy denote the number of gravity stations in the x and y directions, while nbz is the number of blocks in the (depth) z direction. $padx$ and $pady$ denote the numbers of cells which may added around the gravity data grid in x and y directions, respectively.

Here we use the standard notation that vector $\mathbf{d} \in \mathcal{R}^m$ is the set of measurements given by the g_i, and $\mathbf{m} \in \mathcal{R}^n$ is the vector of unknown model parameters.

Practical geophysical data are always contaminated by noise. Suppose that $\mathbf{e} \in \mathcal{R}^m$ represents the error in the measurements, assumed to be Gaussian and uncorrelated, then (5) is replaced by

$$\mathbf{d}_{\text{obs}} = G\mathbf{m} + \mathbf{e}. \tag{6}$$

The purpose of the gravity inverse problem is to find a geologically plausible density model $\mathbf{m}$ that reproduces $\mathbf{d}_{\text{obs}}$ at the noise level.

3 Focusing inversion methodology

An approximate solution for the ill-posed inverse problem described by (6) can be obtained by minimizing the penalized least squares Tikhonov functional defined by

$$\mathbf{m}(\alpha) := \arg\min_{\mathbf{m}} \{\|W_{\mathbf{d}}(G\mathbf{m} - \mathbf{d}_{\text{obs}})\|_2^2 + \alpha^2 \|D(\mathbf{m} - \mathbf{m}_{\text{apr}})\|_2^2\}. \tag{7}$$

Here $\|W_{\mathbf{d}}(G\mathbf{m}-\mathbf{d}_{\text{obs}})\|_2^2$ is the weighted data fidelity and $\|D(\mathbf{m}-\mathbf{m}_{\text{apr}})\|_2^2$ is the regularization term. Data weighting matrix is given by $W_{\mathbf{d}} = \text{diag}(1/\eta_1, \ldots, 1/\eta_m)$, where η_i is the standard deviation of the noise in the ith datum. $G\mathbf{m}$ is the vector of predicted data, D is the regularization matrix and $\mathbf{m}_{\text{apr}}$ is a given reference vector of a priori information for the model $\mathbf{m}$. In (7) α is a regularization parameter which trades-off between the data fidelity and regularization terms. Introducing $\tilde{G} := W_{\mathbf{d}}G$ and $\tilde{\mathbf{d}}_{\text{obs}} := W_{\mathbf{d}}\mathbf{d}_{\text{obs}}$ in order to whiten the noise in the measurements $\mathbf{d}_{\text{obs}}$, and shifting by the prior information through $\mathbf{y} = \mathbf{m}-\mathbf{m}_{\text{apr}}$, we find instead

$$\mathbf{y}(\alpha) := \arg\min_{\mathbf{y}}\{\|\tilde{G}\mathbf{y} - \tilde{\mathbf{r}}\|_2^2 + \alpha^2\|D\mathbf{y}\|_2^2\}, \quad \tilde{\mathbf{r}} = (\tilde{\mathbf{d}}_{\text{obs}} - \tilde{G}\mathbf{m}_{\text{apr}}). \tag{8}$$

Under the assumption that the null spaces of $\tilde{G}$ and D do not intersect, $\mathbf{m}(\alpha)$ is explicitly dependent on α and is defined in terms of the regularized inverse $\tilde{G}(\alpha)$,

$$\mathbf{y}(\alpha) = (\tilde{G}^T\tilde{G} + \alpha^2 D^T D)^{-1}\tilde{G}^T\tilde{\mathbf{r}} = \tilde{G}(\alpha)\tilde{\mathbf{r}}, \quad \tilde{G}(\alpha) := (\tilde{G}^T\tilde{G} + \alpha^2 D^T D)^{-1}\tilde{G}^T \tag{9}$$

$$\mathbf{m}(\alpha) = \mathbf{m}_{\text{apr}} + \mathbf{y}(\alpha) = \mathbf{m}_{\text{apr}} + \tilde{G}(\alpha)\tilde{\mathbf{r}}. \tag{10}$$

It is well-known that when the matrix D is invertible the standard form transformation, [6], yields the alternative but equivalent formulation

$$(\tilde{G}^T\tilde{G} + \alpha^2 D^T D) = D^T((D^T)^{-1}\tilde{G}^T\tilde{G}D^{-1} + \alpha^2 I_n)D. \tag{11}$$

The system describing the fidelity is replaced by the right preconditioned matrix $\tilde{\tilde{G}} := \tilde{G}D^{-1}$, giving the regularized inverse $\tilde{\tilde{G}}(\alpha) := (\tilde{\tilde{G}}^T\tilde{\tilde{G}}+\alpha^2 I_n)^{-1}\tilde{\tilde{G}}^T$, for which $\mathbf{z}(\alpha) = D\mathbf{y}(\alpha)$ is defined by

$$\mathbf{z}(\alpha) := \arg\min_{\mathbf{z}}\{\|\tilde{\tilde{G}}\mathbf{z} - \tilde{\mathbf{r}}\|_2^2 + \alpha^2\|\mathbf{z}\|_2^2\}. \tag{12}$$

Thus

$$\mathbf{m}(\alpha) = \mathbf{m}_{\text{apr}} + D^{-1}\mathbf{z}(\alpha). \tag{13}$$

Although analytically equivalent, numerical techniques to find (10) and (13) differ, for example using for (10) the generalized singular value decomposition, e.g. [15], for the matrix pair $[\tilde{G}, D]$, but the SVD of the $\tilde{\tilde{G}}$ for (13), e.g.[5]. The solutions depend on the stability of these underlying decompositions, as well as the feasibility of calculating D^{-1}.

Practically, the gravity inversion problem solves (7) with an iteratively-defined operator, $D^{(k)} \in \mathcal{R}^{n\times n}$ given by the product $D^{(k)} = W_{\text{e}}^{(k)} W_{\text{depth}} W_{\text{hard}}$. While the depth weighting matrix [10], $W_{\text{depth}} = \text{diag}(1/(z_j)^{\beta})$, and the hard constraint matrix, W_{hard} are independent of the iteration index, the MS stabilizer matrix [16], depends on the iteration. Specifically, $W_{\text{e}}^{(k)} = \text{diag}\left((\mathbf{m}^{(k)} - \mathbf{m}^{(k-1)})^2 + \epsilon^2\right)^{-1/2}$, $k > 0$, with $W^{(0)} = I$ and $\mathbf{m}^{(0)} = \mathbf{m}_{\text{apr}}$, see [18]. The parameter $\epsilon > 0$ is a focusing parameter which provides stability as $\mathbf{m}^{(k)} \to \mathbf{m}^{(k-1)}$ and parameter β determines the weight on the cell j with mean depth z_j. The hard constraint matrix W_{hard} is initialized as the identity matrix, with $(W_{\text{hard}})_{jj} = H$, where H is a large number which then forces $(\mathbf{m}_{\text{apr}})_j = \rho_j$ for those j where geological and geophysical information are able to provide the value of the density of cell j. In order to recover a feasible image of the subsurface lower and upper density bounds $[\rho_{\min}, \rho_{\max}]$ are imposed. During the inversion process if a given density value falls outside the bounds, the value at that cell is projected back to the nearest constraint value. Furthermore, the algorithm terminates when the solution either reaches the noise level, i.e. $\chi^2_{\text{Computed}} := \|(\mathbf{d}_{\text{obs}})_i - (\mathbf{d}_{\text{pre}})_i/\eta_i\|_2^2 \leq m + \sqrt{2m}$, or a maximum number of iterations is reached.

The iterative formulation of (12), given $\{\alpha^{(k)}, k > 0\}$, is now clear. We set regularizer $D^{(k)} = D(\mathbf{m}^{(k)}, \mathbf{m}^{(k-1)})$ and $\tilde{\mathbf{r}}^{(k)} = \mathbf{d}_{\text{obs}} - \tilde{G}\mathbf{m}^{(k)}$ for $k > 1$, initialized with $\tilde{\mathbf{r}}^{(0)} = \mathbf{d}_{\text{obs}} - \tilde{G}\mathbf{m}_{\text{apr}}$ and $D^{(0)} = W_{\text{depth}}$, yielding the regularization parameter dependent updates

$$\mathbf{z}(\alpha^{(k+1)}) = (\tilde{\tilde{G}}^T\tilde{\tilde{G}} + (\alpha^{(k)})^2 I_n)^{-1}\tilde{\tilde{G}}\tilde{\mathbf{r}}^{(k)}, \tag{14}$$

$$\mathbf{m}^{(k+1)} = \mathbf{m}^{(k)} + (D^{(k+1)})^{-1}\mathbf{z}(\alpha^{(k+1)}). \tag{15}$$

Using the SVD for the matrix $\tilde{\tilde{G}}$, see A, (14) can be written as

$$\mathbf{z}(\alpha^{(k+1)}) = \sum_{i=1}^{m} \frac{\sigma_i^2}{\sigma_i^2 + (\alpha^{(k)})^2} \frac{\mathbf{u}_i^T\tilde{\mathbf{r}}^{(k)}}{\sigma_i}\mathbf{v}_i \tag{16}$$

This formulation (16) demonstrates that we may efficiently accomplish the solver through use of the SVD in place of the GSVD.

Still, the algorithm suggested by (14)-(15) also requires estimation of the parameter $\alpha^{(k)}$ which further complicates the solution process. First, an approach for determining or describing an optimal α must be adopted and rationalized. Second, regardless of the criterion that is chosen for finding α, the implementation requires calculating $\mathbf{m}(\alpha)$ for multiple choices of α. It is therefore crucial to have an effective criterion for defining an optimal α at each step.

4 Regularization parameter estimation

Effective and efficient regularization parameter estimation for Tikhonov regularization is well-described in the literature e.g. [6, 20]. In the context of the gravity inversion problem the regularization parameter α is required at each iteration k, and thus the problem of finding the *optimal* $\alpha := \alpha_{\text{opt}}$ efficiently is even more crucial. One approach that has been previously adopted in the literature is an iterated Tikhonov procedure in which $\alpha^{(k)}$ is chosen to converge geometrically, e.g. $\alpha^{(k)} = \alpha^{(1)} q^{(k)}$ for a decreasing geometric sequence $q^{(k)}$, e.g. $q^{(k)} = 2^{-k}$, [17, 21], hence eliminating the need to estimate the parameter for other than the first step. Our results will show that this would not be useful here. Assuming then that α is updated each step, the most often used method for potential field data inversion is the MDP. Yet it is well-known that the MDP always leads to an over estimation of the regularization parameter, e.g. [8], and hence an over smoothing of the solution. Further, the LC and GCV are techniques which extend easily for underdetermined systems, without any additional analysis, and were therefore considered in [18]. On the other hand, the UPRE and χ^2 techniques were developed for the solution of underdetermined problems, extending prior results for consistent or overdetermined systems, and carefully validated for their use in 2D focusing inversion [19]. These results indicate a preference for the UPRE and χ^2 techniques. Thus here we focus on the comparison of the established MDP with the UPRE and χ^2 techniques for 3D potential field data inversion. Because the UPRE and χ^2 techniques are less well-known for this problem domain, we briefly describe the rationale for the UPRE and χ^2 techniques, but leave the presentation of the formulae to B and point to [19] for the derivations. We note that as with the MDP, it is assumed that an estimate of the noise level in the data is provided.

4.1 Unbiased predictive risk estimator

Noting that the optimal α_{opt} should minimize the error between the Tikhonov regularized solution $\mathbf{z}(\alpha)$ and the exact solution $\mathbf{z}_{\text{exact}}$, the purpose is to develop a method for effectively estimating this optimal α without knowledge of $\mathbf{z}_{\text{exact}}$ through use of the measurable residual and the statistical estimator of the mean squared norm of the error, [20]. Specifically, with $H(\alpha) = \tilde{\tilde{G}}\tilde{\tilde{G}}(\alpha)$, the predictive error $\mathbf{p}(\mathbf{z}(\alpha))$ given by

$$\mathbf{p}(\mathbf{z}(\alpha)) \;:= \tilde{\tilde{G}}\mathbf{z}(\alpha) - \tilde{\mathbf{r}}_{\text{exact}} = \tilde{\tilde{G}}\tilde{\tilde{G}}(\alpha)\tilde{\mathbf{r}} - \tilde{\mathbf{r}}_{\text{exact}} = (H(\alpha) - I_m)\tilde{\mathbf{r}}_{\text{exact}} + H(\alpha)\tilde{\mathbf{e}}, \tag{17}$$

is not available, but the residual

$$R(\mathbf{z}(\alpha)) := \tilde{\tilde{G}}\mathbf{z}(\alpha) - \tilde{\mathbf{r}} = (H(\alpha) - I_m)\tilde{\mathbf{r}} = (H(\alpha) - I_m)(\tilde{\mathbf{r}}_{\text{exact}} + \tilde{\mathbf{e}}), \tag{18}$$

is measurable. Thus an estimate of the mean squared norm

$$\frac{1}{m}\|\mathbf{p}(\mathbf{z}(\alpha))\|_2^2 \;=\; \frac{1}{m}\|(H(\alpha) - I_m)\tilde{\mathbf{r}}_{\text{exact}} + H(\alpha)\tilde{\mathbf{e}}\|_2^2, \tag{19}$$

is obtained via the mean squared norm for $R(\mathbf{z}(\alpha))$ and some algebra that employs the Trace Lemma [20]. Then, the optimal regularization parameter is selected such that

$$\alpha_{\text{opt}} = \arg\min_{\alpha}\{\frac{1}{m}\|\mathbf{p}(\mathbf{z}(\alpha))\|_2^2\} = \arg\min_{\alpha}\{U(\alpha)\}, \tag{20}$$

where

$$U(\alpha) = \|\tilde{\tilde{G}}\mathbf{z}(\alpha) - \tilde{\mathbf{r}}\|_2^2 + 2\text{trace}(H(\alpha)) - m. \tag{21}$$

is the functional to be minimized for the UPRE technique to find α_{opt}. This functional can be evaluated in terms of the SVD, as indicated in (27).

4.2 χ^2 principle

The χ^2 principle is a generalization of the MDP. Whereas the MDP is obtained under the assumption that α_{opt} should yield a fidelity term that follows a χ^2 distribution with $m-n$ degrees of freedom, for overdetermined systems, the χ^2 principle for regularization parameter estimation considers the entire Tikhonov functional. For weighting of the data fidelity by a known Guassian noise distribution on the measured data and, when the stabilizing term is considered to be weighted by unknown inverse covariance information on the model parameters, the minimum of the Tikhonov functional becomes a random variable that follows a χ^2-distribution with m degrees of freedom, [12, 19], a result that holds also for underdetermined systems, which is not the case for the MDP. Specifically for the MDP one seeks in general

$$\|\tilde{\tilde{G}}\mathbf{z}(\alpha) - \tilde{\mathbf{r}}\|_2^2 = m - n, \quad m \geq n, \tag{22}$$

which is then usually replaced by an estimate based on the variance when $m < n$, see e.g. [4], while for the χ^2 principle we seek

$$P(\mathbf{m}(\alpha)) = \|W_{\mathbf{d}}(G\mathbf{m} - \mathbf{d}_{\text{obs}})\|_2^2 + \alpha^2\|D(\mathbf{m} - \mathbf{m}_{\text{apr}})\|^2 = m, \tag{23}$$

which is under the assumption that $\alpha^2 I$ effectively whitens the noise in the estimate for $\mathbf{m}$ around the mean $\mathbf{m}_{\text{apr}}$. These yield the formulae (26) and (28) for the MDP and χ^2 principle, respectively, when used with the SVD.

5 Synthetic examples

5.1 Synthetic example: Dike

The first model which is used for testing the reliability of the introduced parameter-choice methods is the dipping dike. Figs 2(a)-2(b) show the cross and plane sections of this model. It has density contrast 1 g/cm^3 on an homogeneous background. Simulation data, $\mathbf{d}$, are

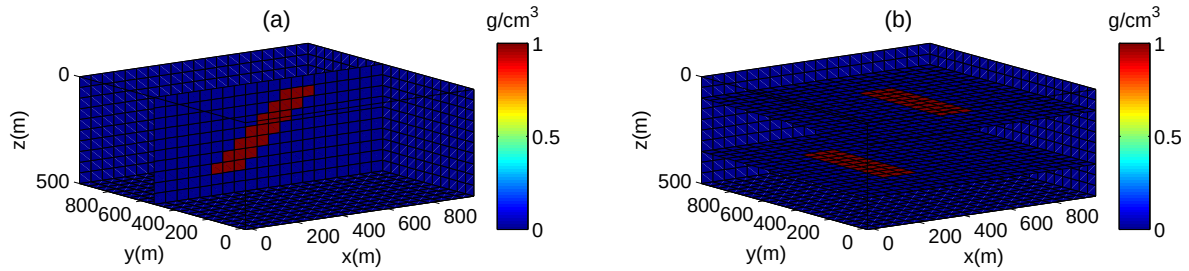

Figure 2: Model of a dipping dike on an homogeneous background. Fig. 2(a): cross-section at $y = 525$ m; Fig. 2(b): plane-sections at $z = 100$ m and $z = 350$ m. The density contrast of the dike is 1 g/cm^3.

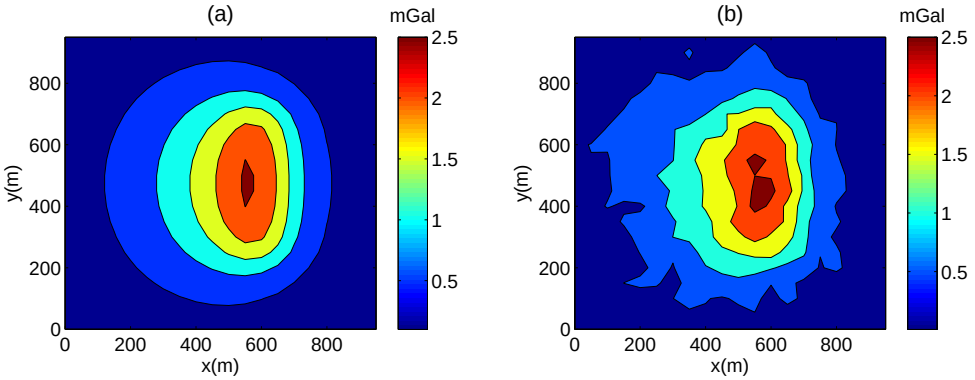

Figure 3: Anomaly due to the dike model shown in Fig. 2. Fig. 3(a): noise free data; Fig. 3(b): data with added noise for $(\eta_1, \eta_2) = (0.02, 0.005)$.

calculated over a 20 by 20 grid with $\Delta = 50$ m on the surface, Fig. 3(a). In generating noise-contaminated data we generate a random matrix Θ of size $m \times 10$ using the MATLAB function **randn**. Then setting $\mathbf{d}^c_{\rm obs} = \mathbf{d} + (\eta_1(\mathbf{d})_i + \eta_2\|\mathbf{d}\|)\Theta^c$, $c = 1 : 10$, generates 10 copies of the right-hand side vector. The inversion results are presented for 3 noise realizations, namely $(\eta_1, \eta_2) = (0.01, 0.001)$; $(\eta_1, \eta_2) = (0.02, 0.005)$; and $(\eta_1, \eta_2) = (0.03, 0.01)$. Fig. 3(b) shows an example of noise-contaminated data for one right-hand side, here $c = 4$, for the second noise realization.

For inversion the subsurface is divided into $20 \times 20 \times 10 = 4000$ cells each with $\Delta = 50$ m. The iterations are initialized with $\mathbf{m}_{\rm apr} = \mathbf{0}$ and $W_{\rm e} = W_{\rm hard} = I_n$. Realistic bounds on the density are imposed by choosing $\rho_{\rm min} = 0$ g/cm^3 and $\rho_{\rm max} = 1$ g/cm^3. For all inversions the coefficient β in $W_{\rm depth}$ and the focusing parameter ϵ are fixed at 0.8 and 0.02, respectively. The algorithm terminates when $\chi^2_{\rm Computed} \leq 429$ or a maximum number of iterations, K, is reached. Here $K = 100$. The inversion is performed for all noise realization choices given by the (η_1, η_2) pairs, and all 10 random copies of the noise simulation in each case. The following average values are calculated for all 10 simulations in each case: (i) the average regularization parameter at the final value, $\alpha^{(K)}$, (ii) the average number of

Table 1: The inversion results obtained by inverting the data from the dike contaminated with the first noise level, $(\eta_1, \eta_2) = (0.01, 0.001)$, average(standard deviation) over 10 runs.

Method	$\alpha^{(1)}, \gamma = 1.5$	$\alpha^{(K)}$	Relative error	Number of iterations
χ^2 principle	4737	287(4.3)	0.7752(0.0048)	80.8(6.6)
UPRE	4737	63(0.001)	0.7699(0.0050)	58.9(4.8)
MDP	4737	215(8.4)	0.7731(0.0051)	100

Table 2: The inversion results obtained by inverting the data from the dike contaminated with the second noise level, $(\eta_1, \eta_2) = (0.02, 0.005)$, average(standard deviation) over 10 runs..

Method	$\alpha^{(1)}, \gamma = 1.5$	$\alpha^{(K)}$	Relative error	Number of iterations
χ^2 principle	4847	66(6.7)	0.7672(0.0089)	6.2(0.9)
UPRE	4847	17.6(1.0)	0.7662(0.0086)	6.6(0.7)
MDP	4847	47.1(2.9)	0.7808(0.0107)	12.7(2.6)

iterations K required for convergence, and (iii) the average relative error of the reconstructed model,$\|\mathbf{m}_{\text{exact}} - \mathbf{m}^{(K)}\|_2 / \|\mathbf{m}_{\text{exact}}\|_2$. The results are presented in Tables 1 - 3, for parameter estimation using the χ^2 principle, the UPRE method, and the MDP method, respectively. Frequently, in potential field data inversion, the initial value of the regularization parameter is taken to be large [4], i.e. at the first step no parameter choice method is required. We consistently initialize $\alpha^{(1)}$ for all methods using the already known singular values of the matrix $\tilde{\tilde{G}}$. Specifically we take $\alpha^{(1)} = (n/m)^{\gamma}(\max(\sigma_i)/\text{mean}(\sigma_i))$. Our investigations show that γ can be chosen such that $0 \leq \gamma \leq 2$.

The results in Tables 1-3 show that both the χ^2 and MDP methods lead to an overestimate of the regularization parameter as compared to that obtained with the UPRE. On the other hand, with respect to the relative error of the reconstructed model, both the χ^2 and UPRE methods lead to reduced error as compared to the MDP. Furthermore, they both require fewer iterations as compared to the MDP and the cost per iteration for the χ^2 method is cheaper than that for the UPRE, requiring just an efficient root-finding algorithm while the UPRE relies on an estimate of $U(\alpha)$ on a range of α.

To illustrate the results summarized in Tables 1-3, Figs 4-6 provide details for a representative case, sample $c = 4$ for the second noise level, $(\eta_1, \eta_2) = (0.02, 0.005)$. Here Figs 4(a), 4(c), 4(e) show the inverted data in cross section at $y = 525$ m and Figs 4(b), 4(d), 4(f) the

Table 3: The inversion results obtained by inverting the data from the dike contaminated with the third noise level, $(\eta_1, \eta_2) = (0.03, 0.01)$, average(standard deviation) over 10 runs.

Method	$\alpha^{(1)}, \gamma = 1.5$	$\alpha^{(K)}$	Relative error	Number of iterations
χ^2 principle	4886	40.8(5.5)	0.7574(0.0132)	3
UPRE	4886	15.8(6.8)	0.7404(0.0149)	3.1(0.31)
MDP	4886	36.6(12.2)	0.7786(0.0133)	3.1(0.31)

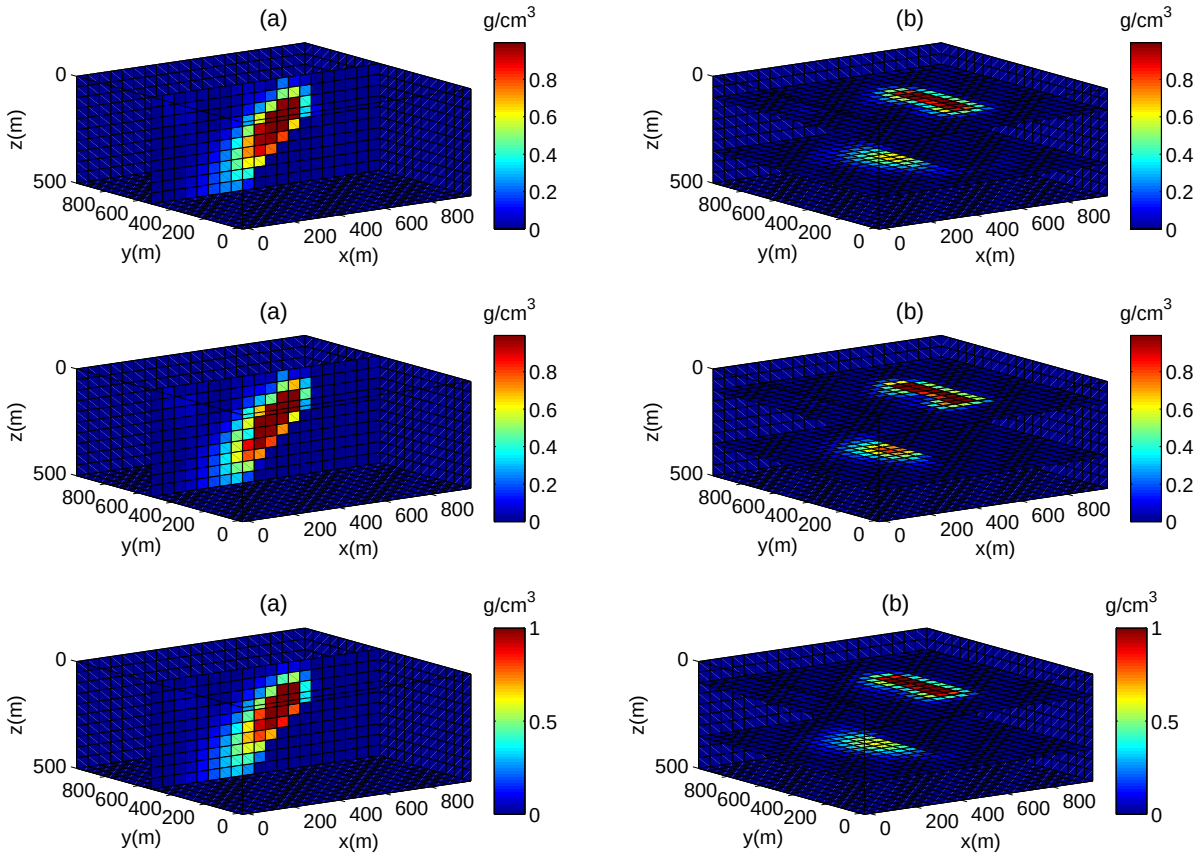

Figure 4: The results obtained by inverting the data shown in Fig. 3(b) using the χ^2 principle, the UPRE and the MDP as the parameter-choice method, respectively. Figs 4(a), 4(c), 4(e): the cross-section at $y = 525$ m in each case, respectively and in Figs 4(b), 4(d), 4(f): the plane-sections at $z = 100$ m and $z = 350$ m for the same cases.

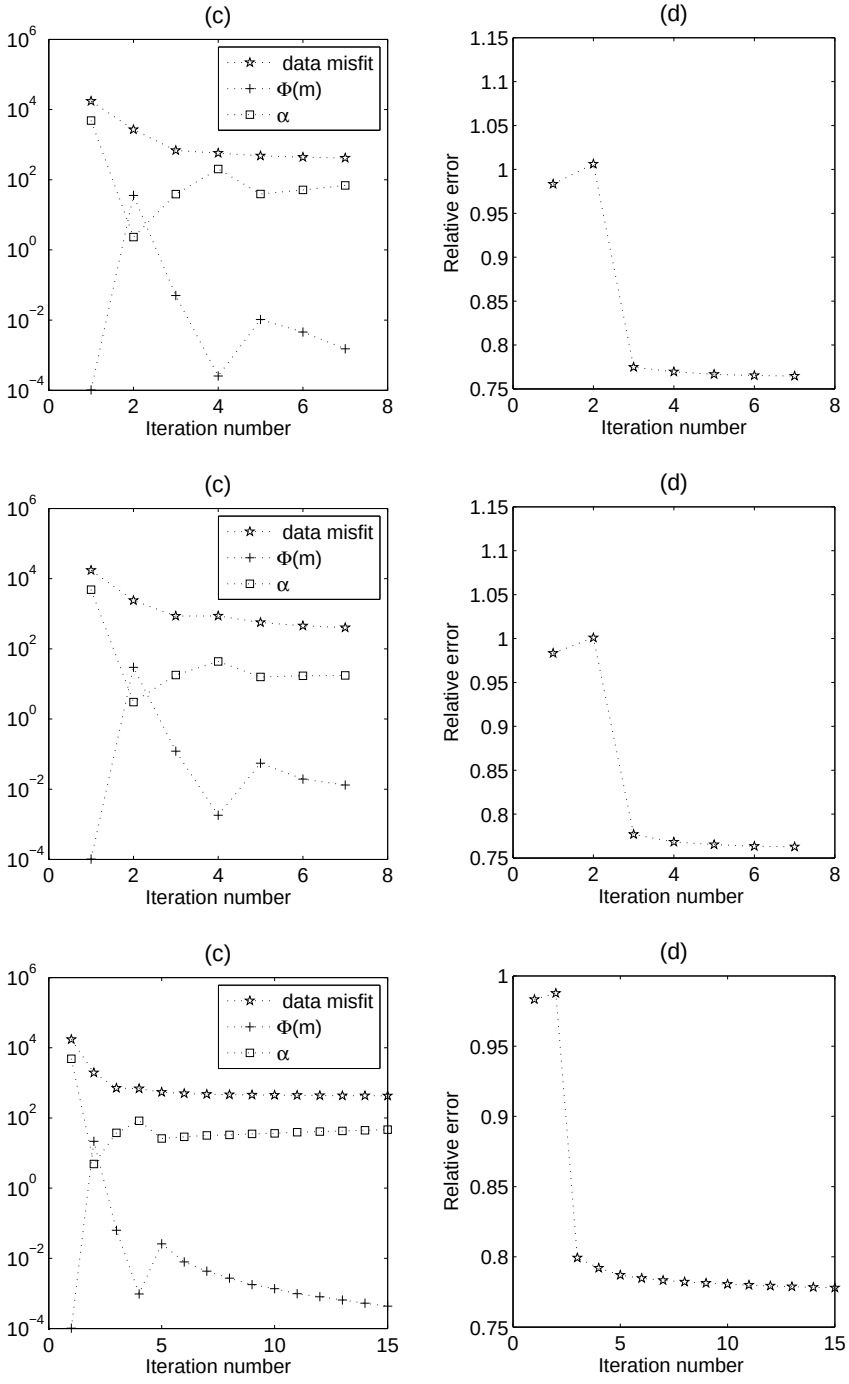

Figure 5: The results obtained by inverting the data shown in Fig. 3(b) using the χ^2 principle, the UPRE and the MDP as the parameter-choice method, respectively. Figs 5(a), 5(c), 5(e): the progression of the data fidelity $\Phi(\mathbf{d}^{(k)})$, the regularization term $\Phi(\mathbf{m}^{(k)})$ and the regularization parameter $\alpha^{(k)}$ with iteration k in each case, respectively and in Figs 5(b), 5(d), 5(f): the progression of the relative error at each iteration for the same cases.

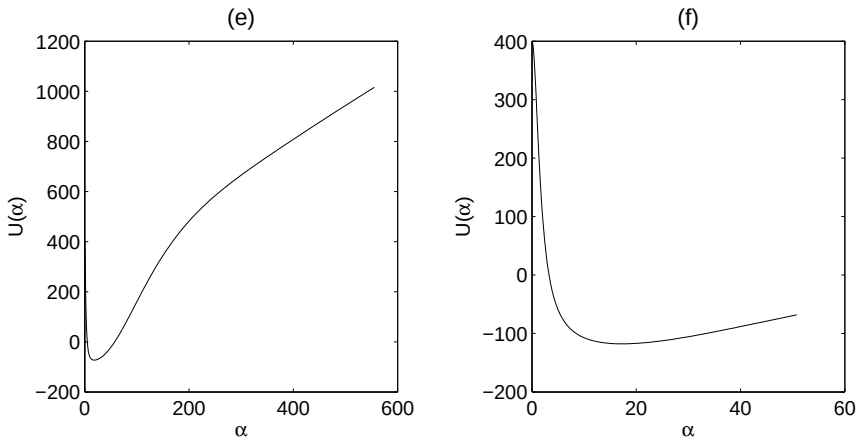

Figure 6: ; Fig. 6(a): the UPRE functional at iteration 3; Fig. 6(b) the UPRE functional at iteration 7.

plane sections at $z = 100$ m and $z = 350$ m. The progression of the data fidelity $\Phi(\mathbf{d}^{(k)})$, the regularization term $\Phi(\mathbf{m}^{(k)})$ and regularization parameter $\alpha^{(k)}$ with iteration k are presented in Figs 5(a), 5(c), 5(e), and in Figs 5(b), 5(d), 5(f) the progression of the relative error. To show that the UPRE functional has a nicely defined minimum we show the functional $U(\alpha)$ at the third and seventh iterations in Figs 6(a)-6(b). In all cases the algorithms produce a dramatic decrease in the relative error by the third iteration, after which the error decreases monotonically, but with a slower rate for the MDP. At the same time the regularization parameter appears to stabilize in each case after the fifth iteration, which is contrary to what one would see by using iterated Tikhonov, which forces the parameter slowly to zero, e.g. [17, 21]. The stabilization observed here suggests that it may be sufficient to carry out the regularization parameter estimation only for a limited number of initial steps, but would require introduction of yet another parameter to assess for stabilization of α. Moreover, further experiments not reported here demonstrate that a dramatic increase in iterations is possible for $\alpha^{(k)}$ not chosen to represent the error levels in the current iteration. Thus, it is important to continue to update α every step of the iteration.

5.2 Synthetic example: Cube

As a second example we choose a cube with dimension 250 m$\times$ 200 m $\times$ 200 m with density contrast 1 g/cm^3 on an homogeneous background, Fig. 7(a). Simulation data, $\mathbf{d}$, are calculated over a 15 by 10 grid with spacing $\Delta = 50$ m on the surface, using the same three noise levels as for the dike simulations. For inversion the subsurface is divided into $15 \times 10 \times 8 = 1200$ cells each of size $\Delta = 50$ m. The simulations are set up as for the case of the dike and the results of the inversions are summarized in Tables 4 - 6, for parameter estimation using the χ^2 principle, the UPRE method, and the MDP method, respectively. An illustration of these results is given in Fig. 7 for the case $c = 5$ for noise level three, $(\eta_1, \eta_2) = (0.03, 0.01)$. These results corroborate the conclusions about the performance of

Table 4: The inversion results obtained by inverting the data from the cube contaminated with the first noise level, $(\eta_1, \eta_2) = (0.01, 0.001)$), average(standard deviation) over 10 runs.

Method	$\alpha^{(1)}, \gamma = 1.5$	$\alpha^{(K)}$	Relative error	Number of iterations
χ^2 principle	1662	98.4(21.8)	0.4144(0.0058)	4.9(0.8)
UPRE	1662	43.6(3.9)	0.4150(0.0055)	4.3(0.5)
MDP	1662	107(4.3)	0.4225(0.0050)	8.1(0.33)

Table 5: The inversion results obtained by inverting the data from the cube contaminated with the second noise level, $(\eta_1, \eta_2) = (0.02, 0.005)$, average(standard deviation) over 10 runs.

Method	$\alpha^{(1)}, \gamma = 1.5$	$\alpha^{(K)}$	Relative error	Number of iterations
χ^2 principle	1688	37.7(5.0)	0.4200(0.0105)	5.3(1.3)
UPRE	1688	18.2(3.0)	0.4225(0.0196)	4.9(0.9)
MDP	1688	36.9(3.6)	0.4202(0.0198)	12.0(2.3)

each method for the dike simulations.

5.3 Solution by the generalized singular value decomposition

In prior work we have used the GSVD to find $\mathbf{z}(\alpha)$ in (12) in place of the SVD as used for the results presented in Sections 5.1-5.2. Here we are not presenting the results using the GSVD. There is no difference in the conclusions that may be deduced concerning the efficacy of the regularization parameter estimators but the GSVD is noticeably more expensive. Indeed there is no difference in the results, i.e. $\alpha^{(K)}$, K and the relative errors are the same, but for a greater computational cost, in our implementation the GSVD algorithm is about 30% more expensive to run. In particular, we note that the standard algorithms for finding a GSVD, first find the SVD of the system matrix $\tilde{G}$. On the other hand, for the implementation using the SVD for $\tilde{\tilde{G}}$ one needs only the SVD and the calculation of the inverse for matrix D which in this case is trivially obtained noting that D is diagonal. It is thus not surprising to find that it is more efficient to use the SVD in place of the GSVD.

Table 6: The inversion results obtained by inverting the data from the cube contaminated with the third noise level, $(\eta_1, \eta_2) = (0.03, 0.01)$, average(standard deviation) over 10 runs.

Method	$\alpha^{(1)}, \gamma = 1.5$	$\alpha^{(K)}$	Relative error	Number of iterations
χ^2 principle	1699	65.4(24.8)	0.4878(0.0324)	4.1(0.33)
UPRE	1699	16.7(2.8)	0.4769(0.0397)	4.1(0.6)
MDP	1699	23.8(6.6)	0.4808(0.0305)	5.9(1.2)

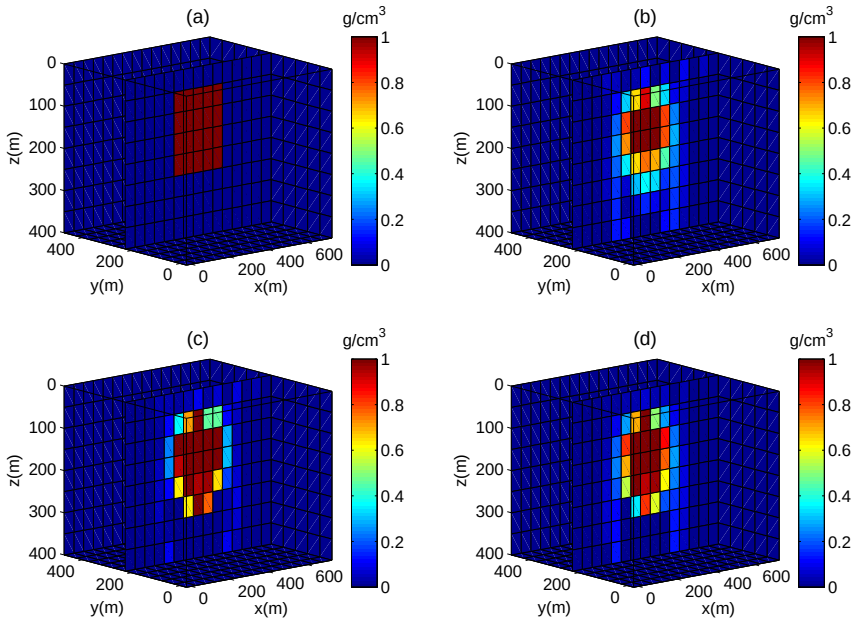

Figure 7: Fig 7(a): Model of a cube on an homogeneous background. The density contrast of the cube is 1 g/cm^3. Fig. 7(b): The density model obtained using the χ^2 principle; Fig. 7(c): The density model obtained using the UPRE; Fig. 7(d): The density model obtained using the MDP.

6 Real data

6.1 Geological context

The field data which is used for modeling are acquired over an area located in the south-west of Iran where a dam, called Gotvand, is constructed on the Karoon river. Tertiary deposits of the Gachsaran formation are the dominant geological structure in the area. It is mainly comprised of marl, gypsum, anhydrite and halite. There are several solution cavities in the halite member of the Gachsaran formation which have outcropped with sink-holes in the area. One of the biggest sink-holes is located in the south-eastern part of the survey area and is called the Boostani sink-hole. The main concern is that it is possible that cavities at the location of the Boostani sink-hole may be connected to several other cavities toward the west and the north and joined to the Karoon river. This can cause a serious leakage of water after construction of the dam or may cause severe damage to the foundations of the dam.

6.2 Residual Anomaly

The gravity measurements were undertaken by the gravity branch of the Institute of Geophysics, Tehran University. Measurements were taken at 1600 stations such that separation between points along the profiles is about 10 m and separation between profiles is 30 m to 50 m. Data were corrected for effects caused by variation in elevation, latitude and topogra-

phy to yield the Bouguer gravity anomaly. The residual gravity anomaly has been computed using a polynomial fitting method, Fig. 8. The six main negative anomalies representing low-density zones are identified on this map. Anomaly 5 is over the Boostani sink-hole. We have selected a box including anomalies 2, 3 and 4 for application of the inversion code, Fig. 9. More details about field procedures, gravity correction and interpretation of the data are provided in [1].

6.3 Inversion results

The residual anomaly, Fig. 9, was sampled every 30 m yielding a box of $32 \times 20 = 640$ gravity points. We suppose that the data is contaminated by error as in the case of the simulations using the noise level case two, $(\eta_1, \eta_2) = (.02, .005)$. The subsurface is divided into $32 \times 20 \times 10 = 6400$ cells of size $\Delta = 30$ m in each dimension. Based on geological information a background density 2.4 g/cm^3 is selected for the inversion and density is limited by $\rho_{\min} = 1.5$ g/cm^3 and $\rho_{\max} = 2.4$ g/cm^3. The results obtained using all three parameter choice methods are collated in Table 7. As for the simulated cases, we find that the final α is larger for both the MDP and χ^2 approaches, suggesting greater smoothing in the solutions. In contrast to the simulated cases, the UPRE requires more iterations to converge, as can be seen in Figs 11(a), 11(b), 11(c), which show the progression of the data fidelity $\Phi(\mathbf{d}^{(k)})$, the regularization term $\Phi(\mathbf{m}^{(k)})$ and the regularization parameter $\alpha^{(k)}$ with iteration k. We stress that the total time for the implementation using the χ^2 principle is about one third of that for the other two methods, requiring in our implementation about 15 minutes as compared to roughly 40 minutes.

In assessing these results, it is also useful to consider the visualizations of the solutions, given in Figs 10(a), 10(c), 10(e), and 10(b), 10(d), 10(f), for the cross sections in the $y - z$ and $x - z$ planes, respectively. Immediate inspection indicates that the solutions using the MDP and χ^2 approach are quite close, while the UPRE differs. Further assessment of the quality of the solutions makes use of our knowledge of the anomalies, the depths of which have been estimated by 3D modeling and are given in Table 8. Fig. 8 also shows that there are two bore holes in the area near anomaly two, for which the range of the low-density zone obtained from these bore-holes is also given in Table 8. Estimations of the same measures of these anomalies using the reconstructions are also collated in Table 8. Now it is clear that indeed the reconstructions using the χ^2 and MDP are very close yielding a range for the density contrast of the low-density zones 2 to 4 of 1.8 to 2.4. On the other hand, the obtained depths using the UPRE are closer to those obtained with the bore-holes, and while the density contrast for anomaly 2 still lies in the interval 1.8 to 2.4, for anomalies 3 and 4 the range is between 1.5 and 2.4. We conclude that the UPRE, although needing now more iterations, is potentially more robust than either of the other methods, but that indeed the χ^2 method can be useful for generating solutions more efficiently, with fewer iterations, and might therefore be used when efficiency is of the highest concern.

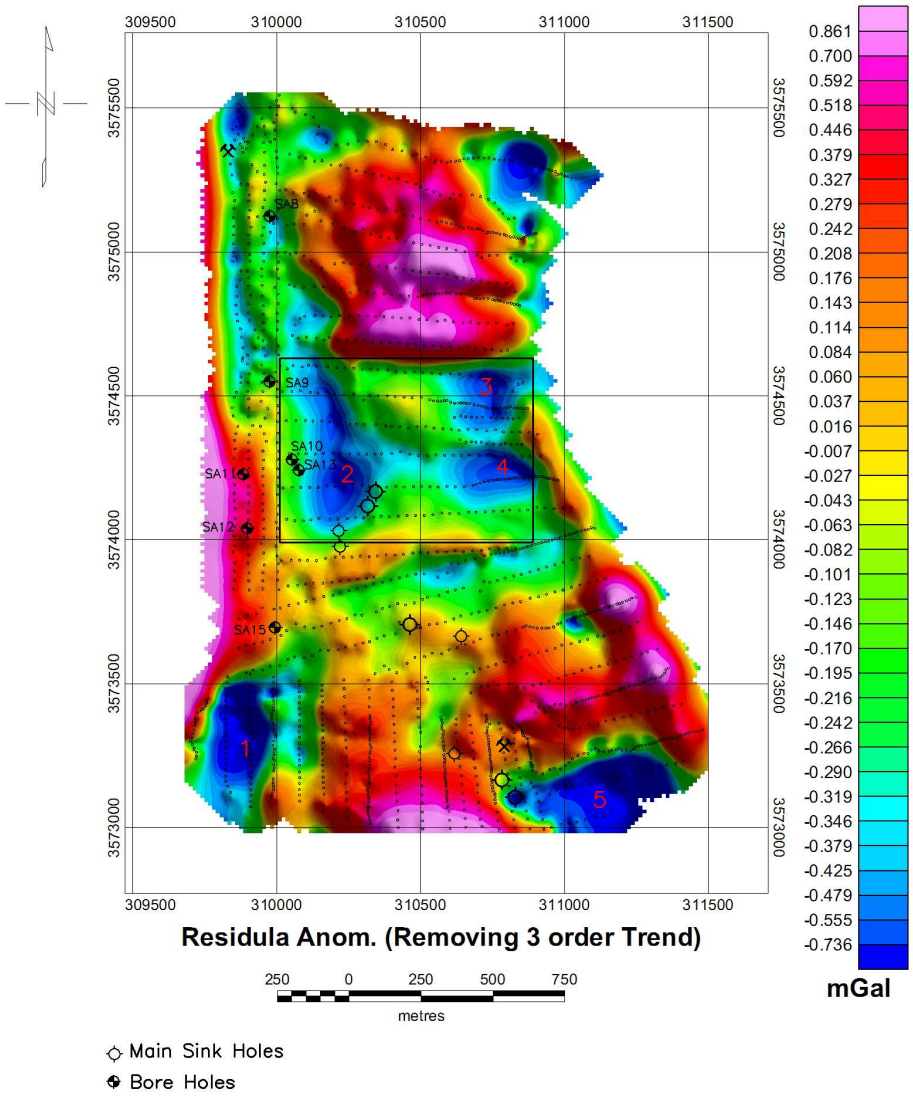

Figure 8: Residual anomaly map over the Gotvand dam site.

Table 7: Results obtained by inverting the data shown in Fig. 9.

Method	$\alpha^{(1)}, \gamma = 1.5$	$\alpha^{(K)}$	Number of iterations
χ^2 principle	5743	51.3	8
UPRE	5743	8.2	29
MDP	5743	44.5	24

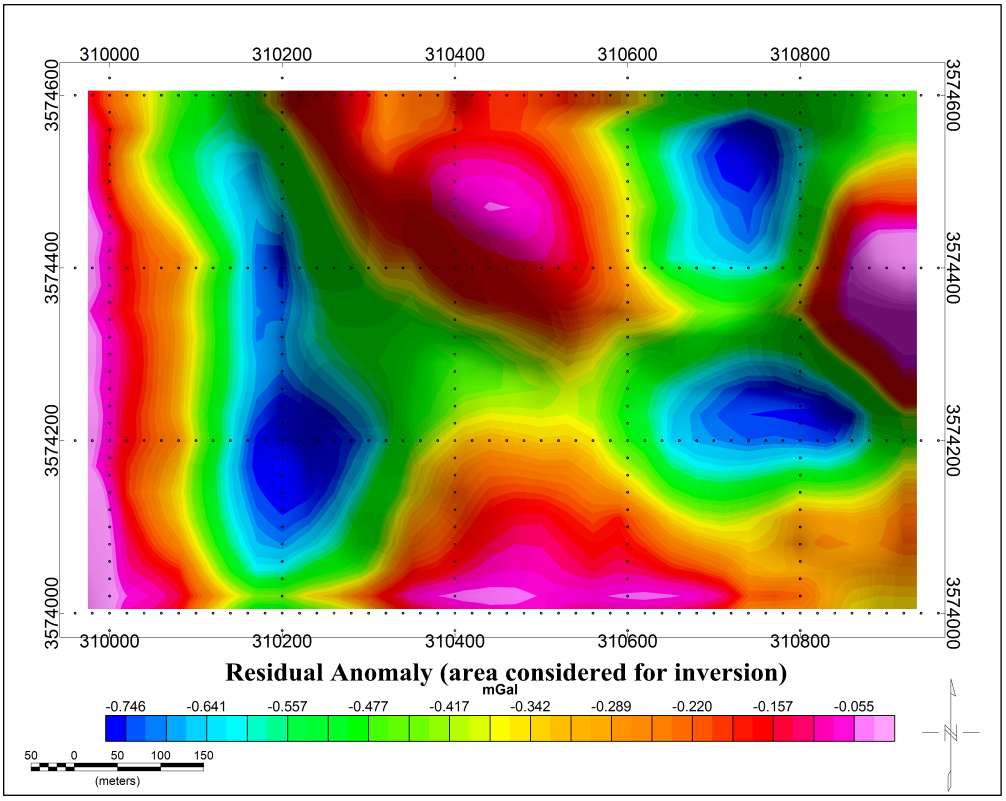

Figure 9: Residual anomaly selected for inversion.

Table 8: Depths obtained using 3D modeling.

Anomaly	χ^2		UPRE		MDP		Bore-hole	
	min	max	min	max	min	max	min	max
2	30-60	150-180	60-90	150	30-60	150-180	115-150	150-160
3	30	90-180	30	90-120	30	90-180	-	-
4	30	150	30	90	30	150	-	-

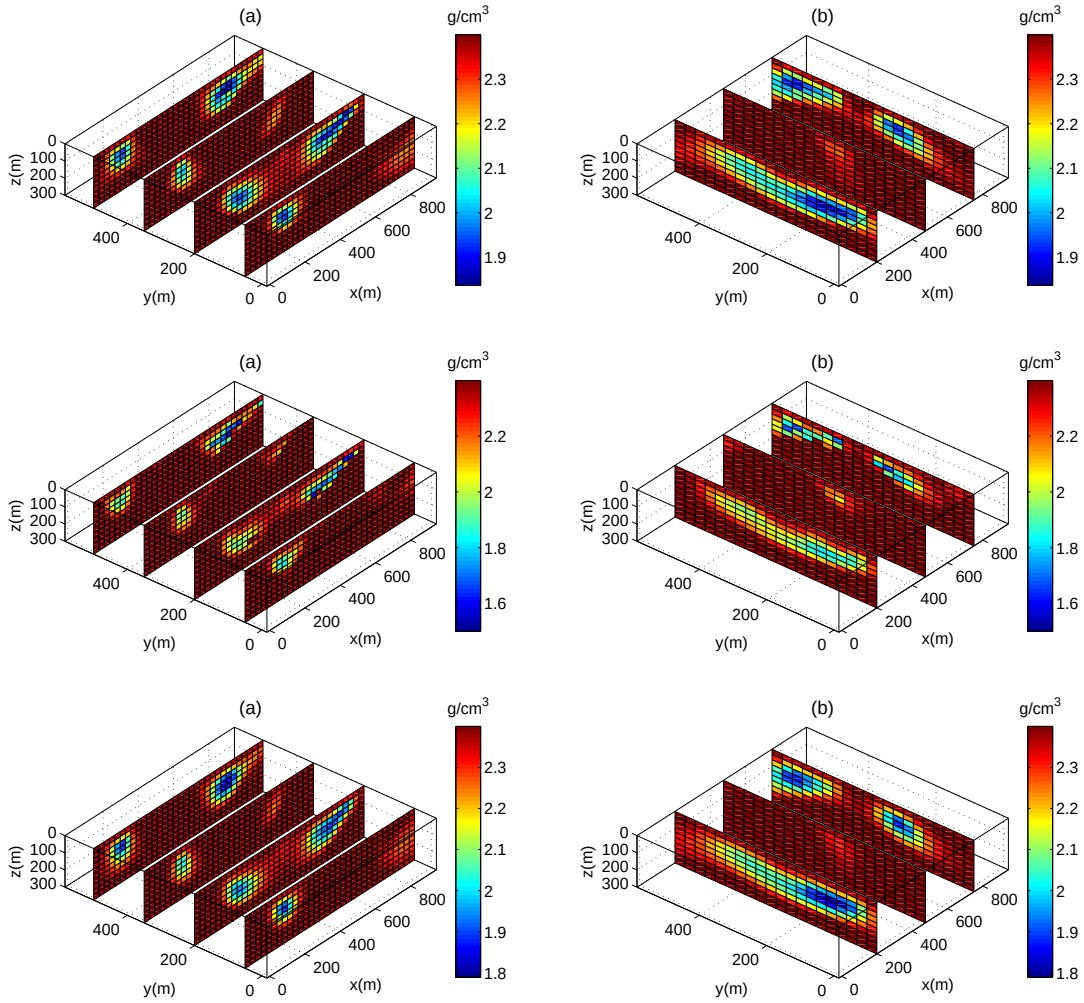

Figure 10: The results obtained by inverting the data shown in Fig. 9 using the χ^2 principle, the UPRE and the MDP as the parameter-choice method, respectively. Figs 10(a), 10(c), 10(e): cross-sections in the $y-z$ plane in each case, respectively and in Figs 10(b), 10(d), 10(f): cross-sections in the $x-z$ plane for the same cases.

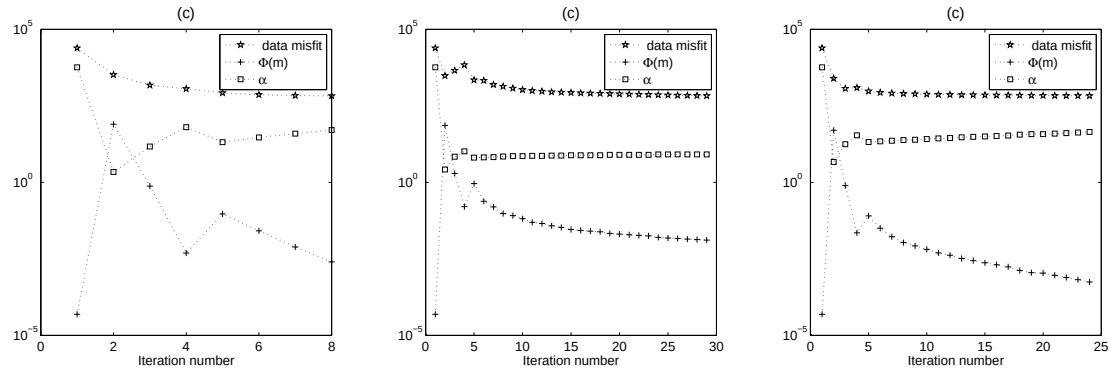

Figure 11: The results obtained by inverting the data shown in Fig. 9 using the χ^2 principle, the UPRE and the MDP as the parameter-choice method, respectively. Figs 11(a), 11(b), 11(c): the progression of the data fidelity $\Phi(\mathbf{d}^{(k)})$, the regularization term $\Phi(\mathbf{m}^{(k)})$ and the regularization parameter $\alpha^{(k)}$ with iteration k in each case, respectively.

7 Conclusions

The χ^2 and UPRE parameter-choice methods have been introduced in the context of 3D gravity modeling. Presented results validate that both methods are more effective than the more often used MDP. While the χ^2 technique is itself very fast for each iteration, requiring only an effective one dimensional root finding algorithm, it also converges quickly. Thus it is definitely to be preferred over the MDP. On the other hand, the UPRE generally provides results with the least relative error in contrast to the MDP and χ^2 methods, particularly for situations with higher noise levels, even if the results for practical data demonstrate that the number of iterations may be increased. In terms of the implementation of the UPRE, the only disadvantage is that finding the optimal α at each step requires the calculation of the $U(\alpha)$ for a range of α. Still we have seen that the minimum of $U(\alpha)$ is well-defined during the iterations.

In these results we have presented an algorithm for finding the minimum of the Tikhonov functional using the SVD for the system matrix in standard form [6] at each iteration in contrast to the use of the GSVD for the augmented matrix formed from the system and stabilizing matrices. The resulting algorithm is much faster and less memory intense, representing generally 30% savings in our implementation. Moreover, it has been successfully validated for the modeling of the subsurface for the Gotvand dam site located in south-west Iran. These results indicate that the low-density zones extend between 60 and 150 m in depth, which is in general agreement with measurements obtained from bore-holes.

While the results here have demonstrated the practicality of the regularization parameter estimation techniques in conjunction with the minimum support stabilizer and the singular value decomposition for 3D focusing gravity inversion, the computational cost per reconstruction is still relatively high. For future work we plan to investigate projected Krylov methods to solve the systems at each iteration. Replacement of the SVD at each step by

an iterative technique is straightforward, but the question of determining the optimal regularization parameter for the solution on the underlying Krylov subspace each step is still an unresolved question and worthy of further study for reducing the cost of 3D inversions in complex environments, as well as for inclusion of alternative edge preserving regularizers.

Acknowledgments

Rosemary Renaut acknowledges the support of AFOSR grant 025717: "Development and Analysis of Non-Classical Numerical Approximation Methods", and NSF grant DMS 1216559: "Novel Numerical Approximation Techniques for Non-Standard Sampling Regimes".

A The singular value decomposition

The solution of the regularized problem defined by right preconditioned matrix $\tilde{\tilde{G}}$ uses the singular value decomposition (SVD) of the matrix $\tilde{\tilde{G}}$. Matrix $\tilde{\tilde{G}} \in \mathcal{R}^{m\times n}$, $m < n$, is factorized as $\tilde{\tilde{G}} = U\Sigma V^T$. The singular values are ordered $\sigma_1 \geq \sigma_2 \geq \cdots \geq \sigma_m > 0$ and occur on the diagonal of $\Sigma \in \mathcal{R}^{m\times n}$ which has $n-m$ zero columns, [5]. Matrices $U \in \mathcal{R}^{m\times m}$ and $V \in \mathcal{R}^{n\times n}$ are row and column orthonormal. Then the solution of the regularized problem with parameter α is

$$\mathbf{z}(\alpha) = \sum_{i=1}^{m} \frac{\sigma_i^2}{\sigma_i^2+\alpha^2}\frac{\mathbf{u}_i^T\tilde{\mathbf{r}}}{\sigma_i}\mathbf{v}_i = \sum_{i=1}^{m} f_i(\alpha)\frac{s_i}{\sigma_i}\mathbf{v}_i \quad s_i = \mathbf{u}_i^T\tilde{\mathbf{r}} \tag{24}$$

$$f_i(\alpha) = \frac{\sigma_i^2}{\sigma_i^2+\alpha^2},\ 1 \leq i \leq m, \quad s_i = \mathbf{u}_i^T\tilde{\mathbf{r}}, \tag{25}$$

where $\mathbf{u}_i$ and $\mathbf{v}_i$ are the ith columns of matrices U and V and $f_i(\alpha)$ are the filter factors.

B Regularization parameter estimation

B.1 Morozov discrepancy principle

Using the SVD for $\tilde{\tilde{G}}$, the MDP for finding α solves

$$\sum_{i=1}^{m}\left(\frac{1}{\sigma_i^2\alpha^{-2}+1}\right)^2(\mathbf{u}_i^T\tilde{\mathbf{r}})^2 - m = 0. \tag{26}$$

B.2 Unbiased predictive risk estimator

Regularization parameter α is found to minimize the functional

$$U(\alpha) = \sum_{i=1}^{m}\left(\frac{1}{\sigma_i^2\alpha^{-2}+1}\right)^2(\mathbf{u}_i^T\tilde{\mathbf{r}})^2 + 2\left(\sum_{i=1}^{m} f_i(\alpha)\right) - m. \tag{27}$$

B.3 The χ^2 principle

Parameter α is found as the root of

$$\sum_{i=1}^{m} \left(\frac{1}{\sigma_i^2 \alpha^{-2} + 1} \right) (\mathbf{u}_i^T \tilde{\mathbf{r}})^2 - m = 0. \tag{28}$$

References

[1] Ardestani V E 2013 Detecting, delineating and modeling the connected solution cavities in a dam site via microgravity data *Acta Geodaetica et Geophysica* **48** 123-138

[2] Aster R C, Borchers B and Thurber C H 2013 *Parameter Estimation and Inverse Problems* second edition Elsevier Inc. Amsterdam.

[3] Boulanger O and Chouteau M 2001 Constraint in 3D gravity inversion *Geophysical prospecting* **49** 265-280

[4] Farquharson C G and Oldenburg D W 2004 A comparison of Automatic techniques for estimating the regularization parameter in non-linear inverse problems *Geophys.J.Int* **156** 411-425

[5] Golub G H and van Loan C 1996 *Matrix Computations* (John Hopkins Press Baltimore) 3rd ed.

[6] Hansen P C 1998 *Rank-Deficient and Discrete Ill-Posed Problems: Numerical Aspects of Linear Inversion* SIAM Monographs on Mathematical Modeling and Computation **4** Philadelphia

[7] Hansen P C 2007 *Regularization Tools:A Matlab package for analysis and solution of discrete ill-posed problems Version 4.0 for Matlab 7.3*, Numerical Algorithms, **46**, 189-194, and `http://www2.imm.dtu.dk/~pcha/Regutools/`.

[8] Kilmer M E and O'Leary D P 2001 Choosing regularization parameters in iterative methods for ill-posed problems *SIAM journal on Matrix Analysis and Applications* **22** 1204-1221

[9] Last B J and Kubik 1983 Compact gravity inversion *Geophysics* **48**713-721

[10] Li Y and Oldenburg D W 1996 3-D inversion of magnetic data *Geophysics* **61** 394-408

[11] Li Y and Oldenburg D W 1999 *3D Inversion of DC resistivity data using an L-curve criterion* 69th Ann. Internat. Mtg., Soc. Expl. Geophys. Expanded Abstracts 251-254

[12] Mead J L and Renaut R A 2009 A Newton root-finding algorithm for estimating the regularization parameter for solving ill-conditioned least squares problems *Inverse Problems* **25** 025002 doi: 10.1088/0266-5611/25/2/025002.

[13] Morozov V A 1966 On the solution of functional equations by the method of regularization *Sov. Math. Dokl.* **7** 414-417.

[14] Nabighian, M. N., Ander, M. E., Grauch, V. J. S., Hansen, R. O., Lafehr, T. R., Li, Y., Pearson, W. C., Peirce, J. W., Philips, J. D. & Ruder, M. E., 2005. Historical development of gravity method in exploration, *Geophysics*, **70**, 63-89.

[15] Paige C C and Saunders M A 1981 Towards a generalized singular value decomposition *SIAM Journal on Numerical Analysis* **18** 3 398-405.

[16] Portniaguine O and Zhdanov M S 1999 Focusing geophysical inversion images *Geophysics* **64** 874-887

[17] Tikhonov, A. N. & Arsenin, V. Y., 1977. *Solution of Ill-posed Problems*, Washington Winston & Sons ISBN 0-470-99124-0.

[18] Vatankhah S Ardestani V E and Renaut R A 2014 Automatic estimation of the regularization parameter in 2-D focusing gravity inversion: application of the method to the Safo manganese mine in northwest of Iran *Journal Of Geophysics and Engineering* **11** 045001

[19] Vatankhah S Renaut R A and Ardestani V E 2014 Regularization parameter estimation for underdetermined problems by the χ^2 principle with application to 2D focusing gravity inversion *Inverse Problems* **30** 085002

[20] Vogel C R 2002 *Computational Methods for Inverse Problems* SIAM Frontiers in Applied Mathematics SIAM Philadelphia U.S.A.

[21] Zhdanov, M. S. & Tartaras, E., 2002. Three-dimensional inversion of multitransmitter electromagnetic data based on the localized quasi-linear approximation, *Geophys.J.Int.*, **148**, 506-519.